LA-UR- 98-1098

Approved for public release; distribution is unlimited.

Title: WAVE OPTICS SIMULATION OF ATMOSPHERIC TURBULENCE AND REFLECTIVE SPECKLE EFFECTS IN CO2 DIFFERENTIAL ABSORPTION LIDAR (DIAL)

CONF-980412--

Author(s): D. H. Nelson, CST-1
R. R. Petrin, CST-1
E. P. MacKerrow, XCM
M. J. Schmitt, XCM
C. R. Quick, CST-1
A. Zardecki, NIS-7
W. M. Porch, EES-8
M. Whitehead, CST-6
D. L. Walters, Naval Postgraduate School, Monterey CA

Submitted to: AEROSENSE 98 Meeting, Orlando Fl, April 1998

DISTRIBUTION OF THIS DOCUMENT IS UNLIMITED

MASTER

Los Alamos
NATIONAL LABORATORY

DISCLAIMER

DISCLAIMER

Portions of this document may be illegible in electronic image products. Images are produced from the best available original document.

Wave optics simulation of atmospheric turbulence and reflective speckle effects in CO_2 differential absorption LIDAR (DIAL)

Douglas H. Nelson[a], Roger R. Petrin[a], Edward P. MacKerrow[a], Mark J. Schmitt[a], Charles R. Quick[a], Andrew Zardecki[b], William M. Porch[c], Michael Whitehead[d], and Donald L. Walters[d]

[a]Los Alamos National Laboratory, MS E543, Los Alamos, NM 87545
[b]Los Alamos National Laboratory, MS E541, Los Alamos, NM 87545
[c]Los Alamos National Laboratory, MS D407, Los Alamos, NM 87545
[d]Naval Postgraduate School, Code PH/We, Monterey, CA 93943

ABSTRACT

The measurement sensitivity of CO_2 differential absorption LIDAR (DIAL) can be affected by a number of different processes. We will address the interaction of two of these processes: effects due to beam propagation through atmospheric turbulence and effects due to reflective speckle. Atmospheric turbulence affects the beam distribution of energy and phase on target. These effects include beam spreading, beam wander and scintillation which can result in increased shot-to-shot signal noise. In addition, reflective speckle alone has a major impact on the sensitivity of CO_2 DIAL. The interaction of atmospheric turbulence and reflective speckle is of great importance in the performance of a DIAL system. A Huygens-Fresnel wave optics propagation code has previously been developed at the Naval Postgraduate School that models the effects of atmospheric turbulence as propagation through a series of phase screens with appropriate atmospheric statistical characteristics. This code has been modified to include the effects of reflective speckle. The performance of this modified code with respect to the combined effects of atmospheric turbulence and reflective speckle is examined. Results are compared with a combination of experimental data and analytical models.

Keywords: atmospheric turbulence, laser speckle, beam propagation

1. INTRODUCTION

CO_2 Differential Absorption LIDAR (DIAL) systems propagate a beam over long distances through the atmosphere. Beam energy is reflected from a topographic or other target back to the transmitter/receiver where the return signal is detected. Target induced or reflective speckle refers to a complex interference pattern generated when coherent light is reflected from a surface rough on the scale of the laser wavelength. The size of these speckles may be large relative to the size of the LIDAR receiver. This results in very inaccurate measurements of the amount of light reflected from a rough target. Another problem is atmospheric optical turbulence which has several degrading effects on a laser beam. The beam will experience short term spreading which is observed even in short pulses. It also undergoes beam centroid motion which will contribute to long term spreading. Finally, there is scintillation of the beam resulting in fluctuations in the irradiance profile.

Although each of these two separate phenomena is well known and characterized, we feel the combined process warrants further study. An analytical development of the interaction of these two processes has proven limited in terms of characterizing the electric-field observed at the LIDAR receiver. It is clear another approach to this problem is needed. To this end, we intend to investigate the suitability of a computer simulation which will aid in our study of the combined effects of reflective speckle and atmospheric turbulence.

2. MODEL

Our approach consists of a Huygens-Fresnel wave optics computer simulation which models the effects of atmospheric optical turbulence on the path to the target.[12] A random phase is added to the optical phase at the target to simulate reflective speckle. This distorted phase front is then propagated through a return path which again includes the turbulence effects.

The Huygens-Fresnel wave optics computer simulation uses an N x N array of complex numbers in a plane perpendicular to the propagation axis to represent the electric-field. An initial electric-field with a Gaussian TEM_{00} amplitude (matching, as closely as possible, the characteristics of our real transmitter beam) is used as the input for the propagation simulation. The simulation propagates this initial electric-field by dividing the path from LIDAR platform to target into equal sized steps and applying a phase screen (simulating turbulence) at each step. The expression for the electric-field after a step over a distance Δz is determined from

$$E(n_x, n_y, \Delta z) = IFT\left[\exp\left(i \cdot \pi \cdot \lambda \cdot \Delta z \cdot \left|\hat{f}\right|^2\right) \cdot FT\left[E(n_x, n_y, 0) \cdot \exp\left\{i \cdot \theta(n_x, n_y)\right\}\right]\right], \quad (1)$$

where (n_x, n_y) denotes a pixel location within the transverse two-dimensional array, $E(n_x, n_y, 0)$ is the electric-field at the beginning of the step ($z = 0$), FT is the discrete two-dimensional Fourier transform, $\exp\left(i \cdot \pi \cdot \lambda \cdot \Delta z \cdot \left|\hat{f}\right|^2\right)$ is the Fresnel propagator in frequency space $\hat{f}$, λ is the LIDAR wavelength and IFT is the discrete two-dimensional inverse Fourier transform. The phase screen, $\theta(n_x, n_y)$, is the Fourier transform of an array produced in the spatial frequency domain using the Kolmogorov spectrum with a Gaussian random number distribution. The turbulence induced phase at any pixel location, (n_x, n_y), is also dependent on the level of turbulence and the length of the propagation step.

Once at the target, the electric-field phase is randomized (simulating reflective speckle) through the relation

$$E(n_x, n_y)_{\text{reflected}} = E(n_x, n_y)_{\text{target}} \cdot e^{i \cdot 2\pi \cdot random(n_x, n_y)}, \quad (2)$$

where $E(n_x, n_y)_{\text{target}}$ is the complex electric-field incident on the target after propagation through turbulence, $E(n_x, n_y)_{\text{reflected}}$ is the electric-field reflected from the target and $random(n_x, n_y)$ is a uniformly distributed random number between 0 and 1. A uniformly distributed random number was chosen since this is a good approximation for the phase produced by a surface rough compared to a wavelength of the coherent light on the target.[10] The reflected electric-field is then propagated back to the telescope/receiver with turbulence effects induced using the same phase screens as the path out. The return signal is then analyzed over a number of realizations of turbulence and target phase randomizations.

3. SIMULATION RESULTS AND DISCUSSION

3.1 Atmospheric turbulence effects

The ability of the Huygens-Fresnel wave optics code to simulate the effects of atmospheric optical turbulence is well established.[1] It is, however, instructive to investigate this fact. The simulation has certain limitations which include obeying the Rytov criteria which limits the level of turbulence/length of propagation path that may be used. The Fresnel approximation also provides other limits on the length of the propagation steps. The size of the beam on the target is limited so that one may avoid aliasing effects inherent in Fourier transform techniques. Following are typical results we have achieved.

Figure 1 is an example of irradiance patterns from the simulation for a case of near zero turbulence ($C_n^2=10^{-19}$ $m^{-2/3}$). In Figure 2 we have used a higher level of turbulence ($C_n^2=10^{-14}$ $m^{-2/3}$). The turbulent effect on the beam is readily apparent in the image of Figure 2.

In Figure 3 the long term beam spreading effects (including the effects of short term beam spreading and centroid motion) are compared between the simulation, theory and experiment.[3] Least squares curve fits were made using IGOR to determine the beam parameters from the simulation.[4] Theoretical values for plane wave, spherical wave and beam wave cases were calculated assuming uniform turbulence over a horizontal propagation path and taking system beam parameters into account.[5,6]

3.2 Reflective speckle effects

It is important to establish the validity of our model in simulating reflective speckle. We conducted a number of simulations for near zero turbulence conditions which compared favorably with theory and experiments run over a short path (115 m) to minimize the effects of atmospheric optical turbulence.[7] Figure 4 shows a typical speckle pattern at the receiver from our simulation. The theoretical value of the speckle correlation diameter, D_c, for speckle generated by a Gaussian irradiance pattern on the target is [7]

$$D_c = \frac{2 \cdot \lambda \cdot L}{\pi \cdot w_T} , \tag{3}$$

where λ is the wavelength of the LIDAR pulse, L is the propagation distance from the target to the telescope and w_T is the beam spot size (radius) on the target. Figure 5 is a comparison of the correlation sizes produced by the simulation for near zero turbulence with that predicted by theory. These were calculated by taking the normalized autocovariance of a single shot speckle pattern.[8] The normalized autocovariance is defined as [10]

$$C_{I_N} = \frac{\left\langle (I_1 - \langle I \rangle)(I_2 - \langle I \rangle) \right\rangle}{\sigma_I^2}, \tag{4}$$

where I_1 and I_2 denote the intensities at two different points, σ_I^2 represents the variance of the intensity over the points in the speckle pattern and the angled brackets represent an ensemble average over the speckle pattern. We then estimated the correlation size from the point where the normalized autocovariance function was down to e^{-1}.

The number of these reflective speckle (or integrated intensity) that are collected by a LIDAR receiver assembly plays an important role in the statistics of the return signal. If a small number of speckle are integrated per laser pulse the accuracy of the LIDAR measurement is poor. As the number of speckles integrated per laser pulse increases, the accuracy improves. We have estimated the probability density of return signal intensities using the approximate Gamma distribution developed by Goodman.[9,10] This probability density function (pdf) for the integrated intensity of a speckle pattern, I_o, is then

$$p_{I_o}(I_o) = \begin{cases} \dfrac{1}{\Gamma(M)} \left(\dfrac{M}{< I >} \right)^M I_o{}^{M-1} \exp\left(- M \dfrac{I_o}{< I >} \right), & \text{if } I_o > 0 \\ 0, & \text{otherwise.} \end{cases} \tag{5}$$

The factor M can be interpreted as the number of speckles inside the receiver aperture for an average pulse, $< I >$ is the mean value for the integrated intensity of the speckle pattern and Γ is the gamma function. Examples of this distribution for different values of M are shown in Figure 6. For a point detector, $M = 1$, and Equation (5) simplifies to a negative exponential. If the receiver aperture area is smaller than the speckle correlation area, the value of M is unity. In such an instance, the intensity measured at the aperture will be influenced by a single speckle even if only a small fraction of the speckle is sampled. Values of $M < 1$ therefore have no physical meaning.

We have simulated the returns of 1000 pulses with measured intensity for circular receiver apertures of varying radii. Each pulse had a different random number seed as shown in equation (2) to simulate independent speckle realizations. Assuming linearly polarized light, we estimated the M value through

$$M \approx (S/N)_{rms}^2 , \tag{6}$$

where $(S/N)_{rms}$ is the signal to noise ratio of the intensities, I_o, measured by the receiver aperture. Using this value of M and our simulated value of $< I >$ we estimated the probability density function of our simulated intensities through Equation (5). With this pdf and the maximum and minimum simulated I_o we calculated the desired bin width that

would minimize the bias and variance in a histogram plot of our simulated intensities using MATHCAD.[11,12] Several representative plots resulting from this method are shown in Figure 7 through Figure 9. The error bars are based on the number of counts per bin and the appropriate distribution.[13] IGOR was used to curve fit these plots resulting in a revised value of M. Figure 10 shows excellent agreement between the theoretical M and the simulated signal to noise ratio values.

3.3 Combined Effects

We also simulated the combined effects of atmospheric optical turbulence and reflective speckle. Our interest here is to determine the physical processes at work on our return LIDAR signal.

Figure 11 shows a plot much like that of Figure 5 but which in this case includes "speckle" correlation sizes after a round trip (transmitter to target and back to the receiver) through atmospheric turbulence. Note that for the smaller beam diameters on the target, and hence larger theoretical reflective speckle by Equation (3), the resulting turbulence affected "speckle" are smaller. For this particular LIDAR geometry and the higher level of turbulence simulated, the value of the atmospheric transverse coherence length for a coherent spherical wave, $\rho_o \sim 5.5$ cm. Comparison of this information in Figure 11 suggests that there is a break up of the reflective speckle into atmospheric affected "specklets" on the order of ρ_o.[14]

Figure 12 shows a fitted M curve for a representative distribution of received intensities neglecting atmospheric turbulence for a fairly small diffraction limited beam diameter on target. Figure 13 shows the same LIDAR geometry and receiver size but with a higher level of turbulence. This latter plot indicates that this situation results in a slightly larger value of M and is consistent with our findings as shown in Figure 11. From Equation (6), we surmise that in these goemetries one would expect a higher signal to noise (lower noise) for turbulence levels that result in larger M.

In contrast, Figure 14 shows the measured level of noise (standard deviation of the intensity normalized by the mean intensity) for a fairly large beam diameter on target (small reflective speckle at the receiver). In this case the reflective speckle is fairly small but the noise is higher for higher levels of turbulence. Simulations were run for this particular LIDAR geometry and are displayed in Figure 15. In this latter figure there is a definite trend consistent with noise levels shown in Figure 14. The levels are lower in Figure 15 since all sources of noise are neglected except for reflective speckle (independent realizations) and atmospheric turbulence. Other sources of noise include albedo variations over the target surface, laser pulse energy variations that are not fully accounted for in normalizing the incoming signal, jitter in the transmitter/target, detector noise and blackbody background radiation.[7]

4. CONCLUSIONS

It is clear that for certain LIDAR geometries (large beam on target, small speckle) that atmospheric turbulence is an additional source of noise. More study is required to determine more precisely in which cases atmospheric turbulence creates an additional source of noise and in which cases it results in lower noise. There is also the issue of the relative significance of the relationship between the speckle coherence size and the spherical atmospheric coherence length, ρ_o.

Future work should include analysis of experimental LIDAR return signals over turbulent paths with receivers of varying radii and varying diffraction limited beam diameters on target. The resulting intensity distributions can then be compared with Equation (5). In this way, we can get a reasonable estimate of the average number of speckle measured per pulse and can then discern if there was any break up of the reflective speckle by the atmospheric turbulence. With further validation of our model, we may also explore the relative effect that turbulence on different portions of the propagation path has on the speckle-turbulence interaction.

5. ACKNOWLEDGEMENTS

The authors would like to acknowledge technical assistance from L. John Jolin, Chuck Fite and the team at the Nevada Test Site Spill Test Facility.

The simulations presented here were done using our modified code written in and calculated using MATLAB.[15] The computers used included Dell Workstation 400's with 256 MB RAM and 512 MB RAM operating at 300MHz and a Tatung Ultrasparc 2 dual processor operating at 300 MHz . For complete round trip propagations most simulations were conducted on the Tatung. On this machine, 100 iterations for a 512 x 512 array took ~1.6 hours when 5 phase screens were used. A 1024 x 1024 array with the other specifications being the same took ~8 hours. All simulations assumed a CO_2 wavelength of 10.6 μm.

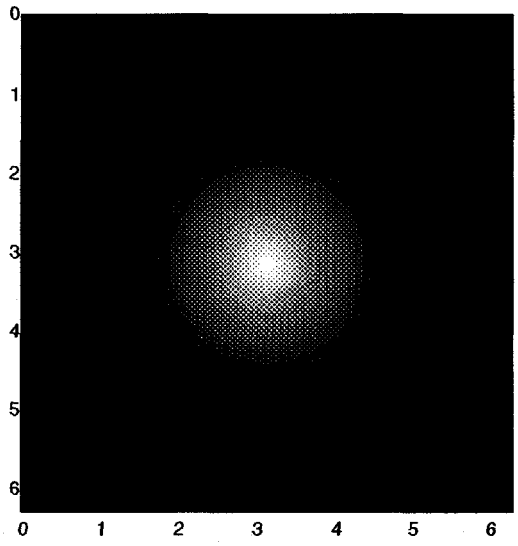

Figure 1. Computer image of Gaussian beam intensity on target with near zero turbulence. Propagation distance is 7300 m and the diffraction limited beam divergence is 0.290 mrad. The simulation used 10 propagation steps of 730 m each with a 512 x 512 array.

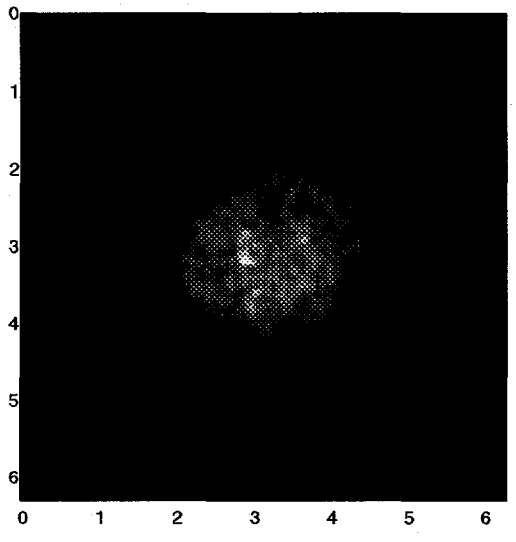

Figure 2. Computer simulated beam intensity on target for a constant $C_n^2=10^{-14}$ $m^{-2/3}$. The simulation parameters are otherwise the same as those used to produce Figure 1. The beam path modeled is horizontal and about 3 m above the ground.

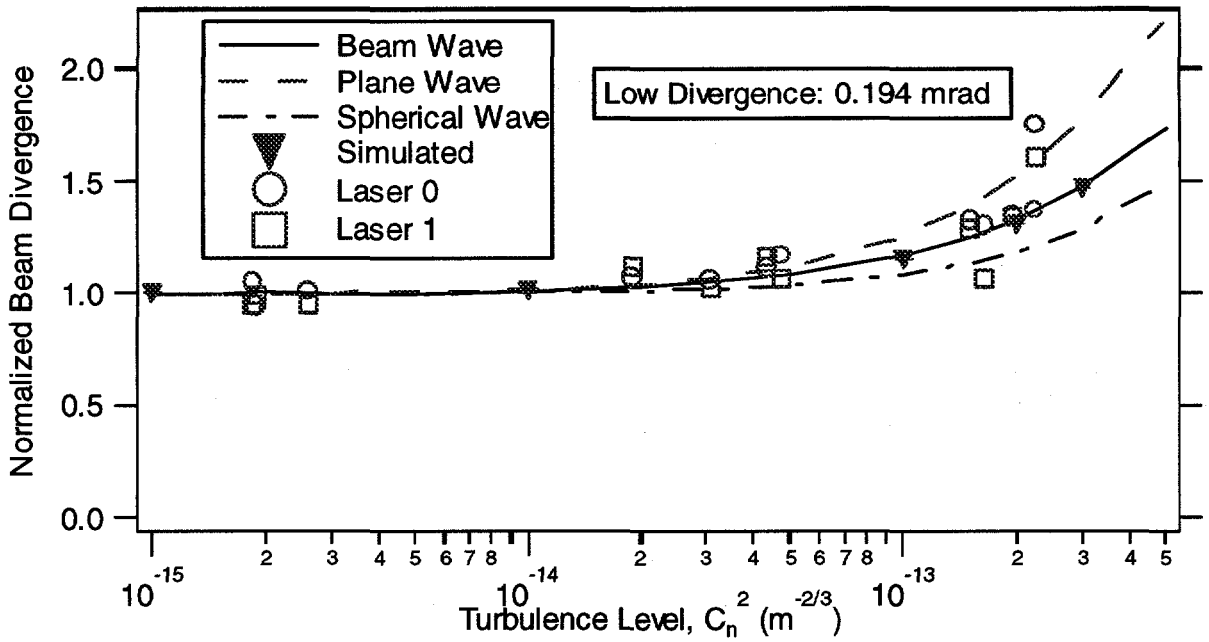

Figure 3. Comparison of experimental and simulation of beam profiling experiment with theory. Beam profile measurements of CO_2 DIAL for a propagation path of 3300 m. Measurements were taken by scanning a pole and determining the best fit Gaussian profile. In the simulation, a total of 100 pulses were summed to give the long term beam spreading effect. Columns of pixels in the resulting pattern were then summed to mimic the effect of scanning a pole resulting in a one dimensional profile. A best fit Gaussian to this resulting profile was determined obtain the beam size. Laser 0 and Laser 1 are the designations used for the two lasers in our system. The simulation used five propagation steps and a 512 x 512 array.

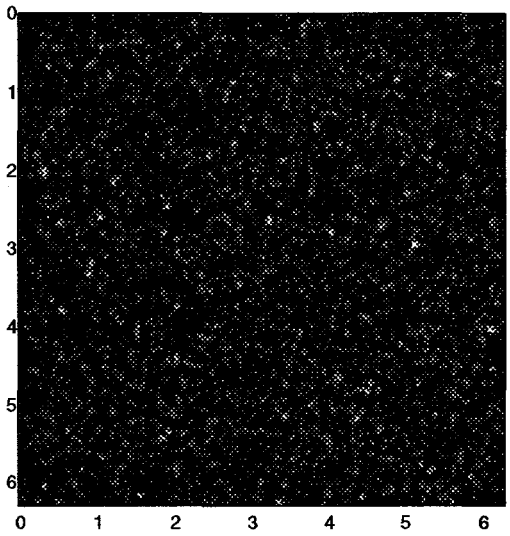

Figure 4. Simulated reflective speckle pattern at the receiver for the case shown in Figure 1 except the beam divergence has been changed to 0.160 mrad.

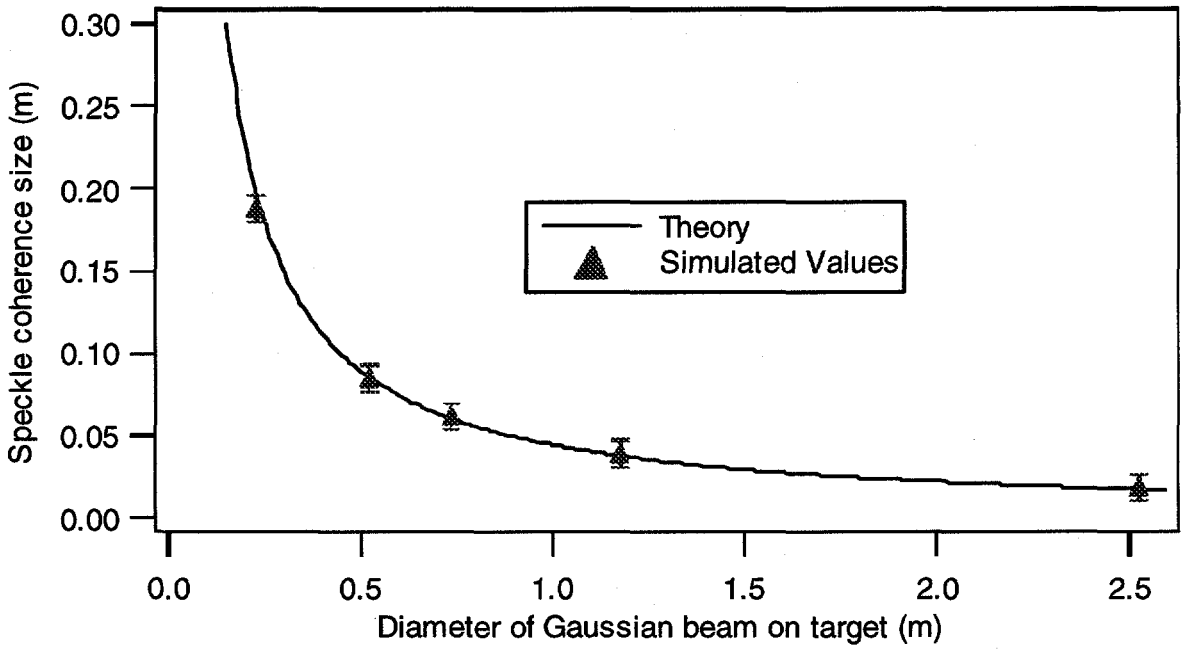

Figure 5. Comparison of simulated speckle size in near zero turbulence with that predicted by theory as a function of beam diameter on target. A single pulse simulation was used with five propagation steps on a 512 x 512 array. The e^{-1} value of the normalized autocovariance rendered the speckle correlation size. The simulated value errors bars represent one pixel width. The theoretical values are given by Equation (3).

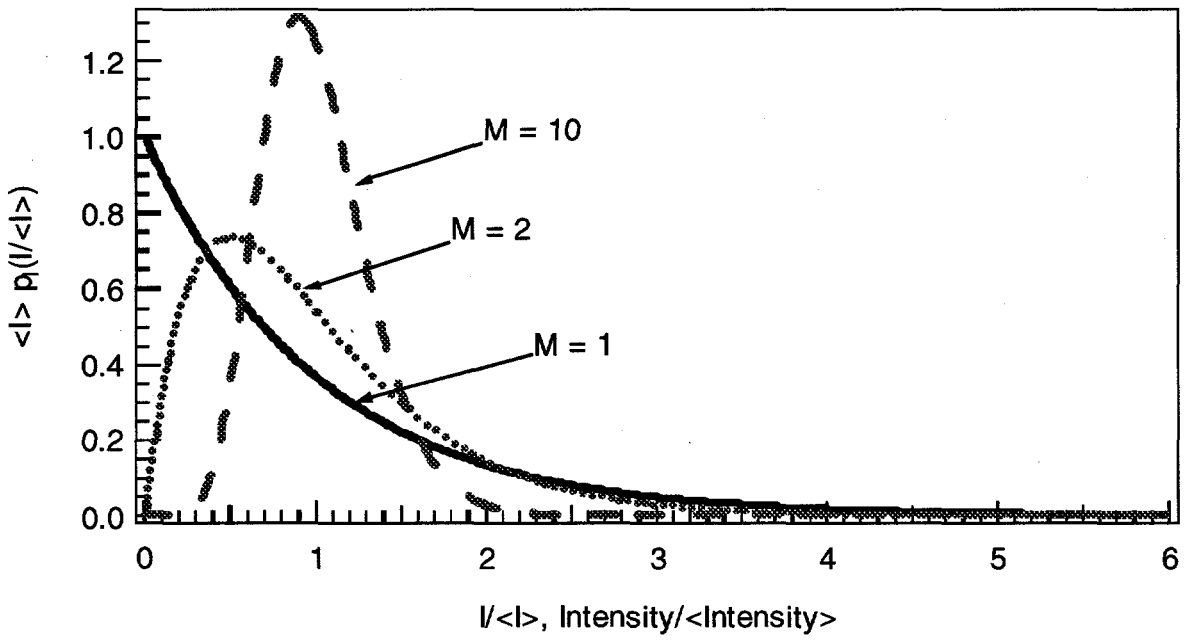

Figure 6. Probability density function for measuring a speckled lidar return of intensity I, Equation (5). M is approximately the number of speckle integrated by the receiver aperture on an average pulse. For M>10 this function approaches a Gaussian probability distribution function.

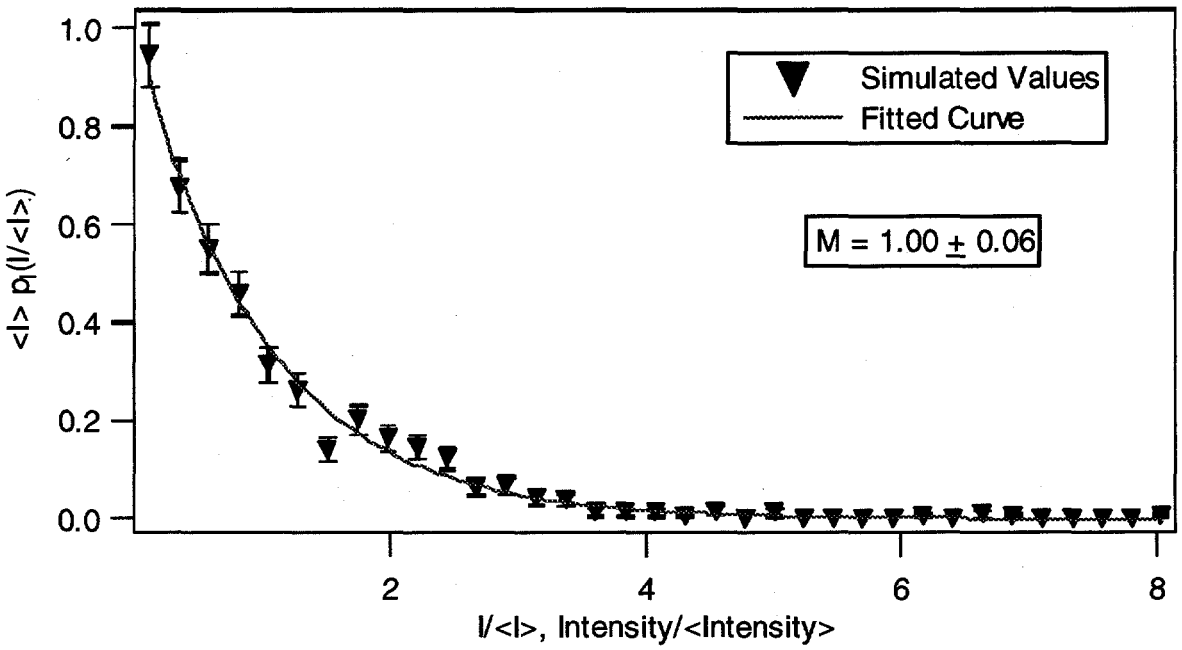

Figure 7. Simulated probability density function for a one pixel (square) receiver of width ~1.2 cm with independent speckle realizations and near zero turbulence ($C_n^2=1\cdot10^{-19}$ $m^{-2/3}$). Diffraction limited diameter of beam on target ~1.17 m. z = 7300 m. The error bars represent the distribution of simulated received intensity for 1000 pulses. The solid curve represents the best fit Gamma. This figure compares favorably with the M = 1 curve in Figure 6. The simulation used 10 propagation steps on a 512 x 512 array.

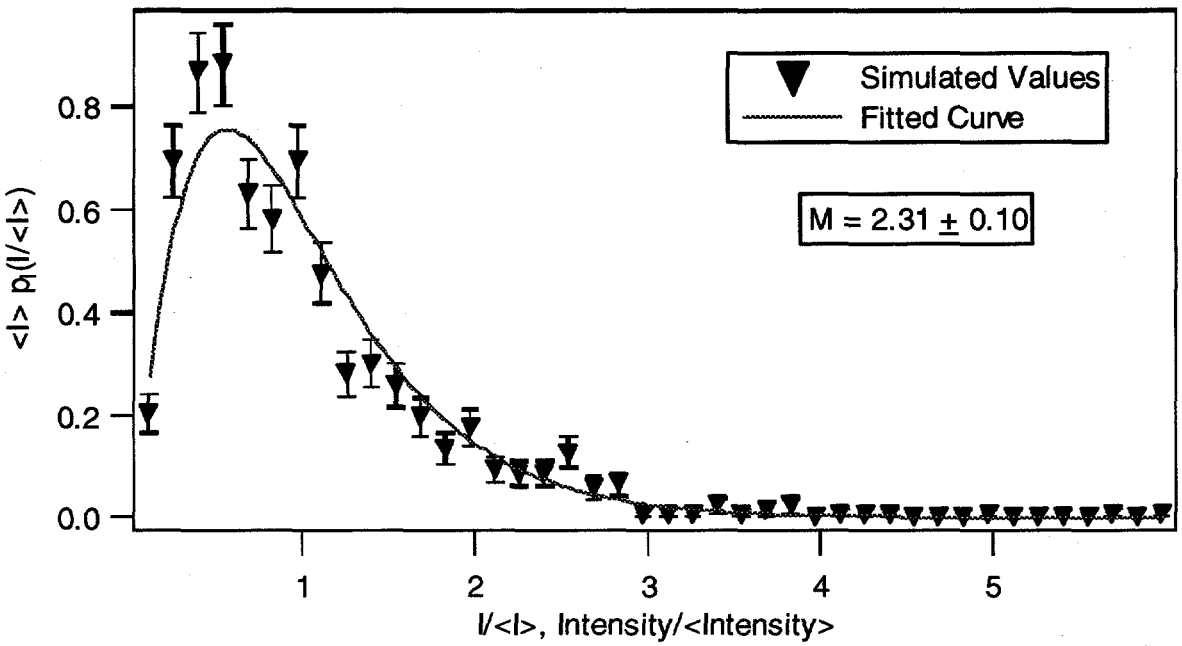

Figure 8. Same simulation parameters as Figure 7 except the receiver radius is ~ 3.7 cm. Note the similarity with the M = 2 curve in Figure 6.

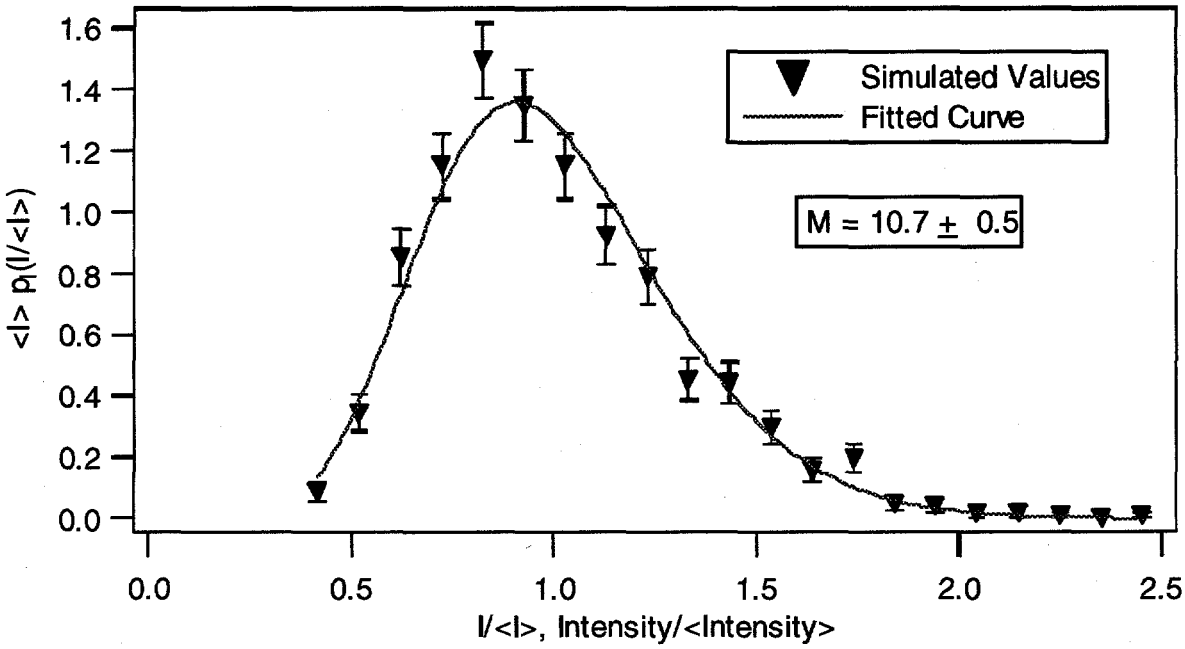

Figure 9. Same simulation parameters as Figure 7 and Figure 8 except the receiver radius is ~ 12.3 cm. The transition to a more Gaussian shape is apparent as with the M = 10 curve in Figure 6.

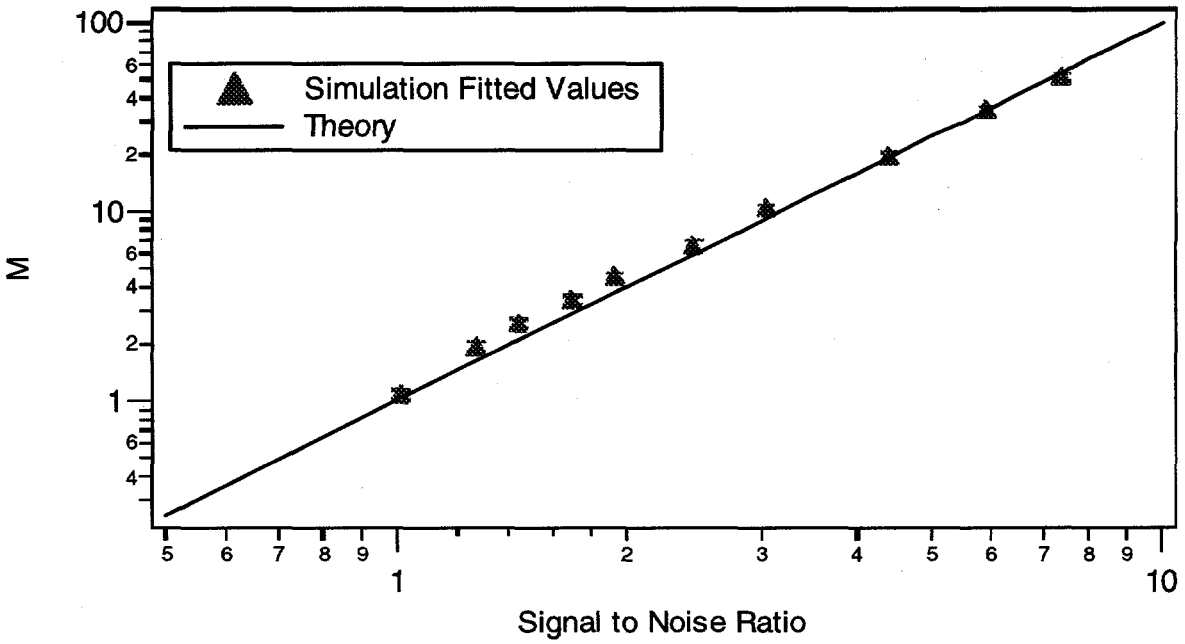

Figure 10. Comparison of fitted M values from simulation and theory versus signal to noise ratio. For this simulation 1000 pulses were simulated for a transmitter to target distance of 3300 m. Five propagation steps on a 512 x 512 array were used. The beam diameter on target ~ 0.74 m. Curve fits were done using IGOR to determine the simulated M factor. The data points represent receiver apertures of different radii.

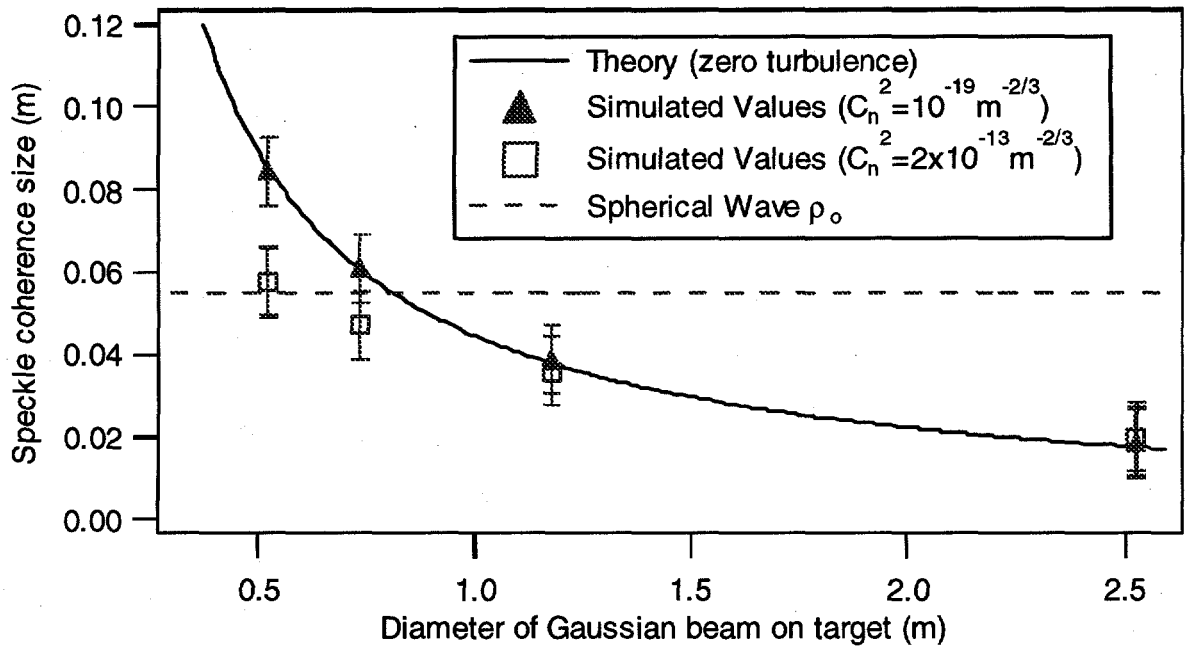

Figure 11. Comparison of simulated speckle size in near zero turbulence and high turbulence with that predicted by theory as a function of beam diameter on target. For smaller beam diameter on target, there is a significant decrease in speckle correlation size for the high turbulence case. For the high turbulence case, the spherical wave atmospheric coherence length, ρ_o, is shown. Propagation range is 3300 m over five steps on a 512 x 512 array.

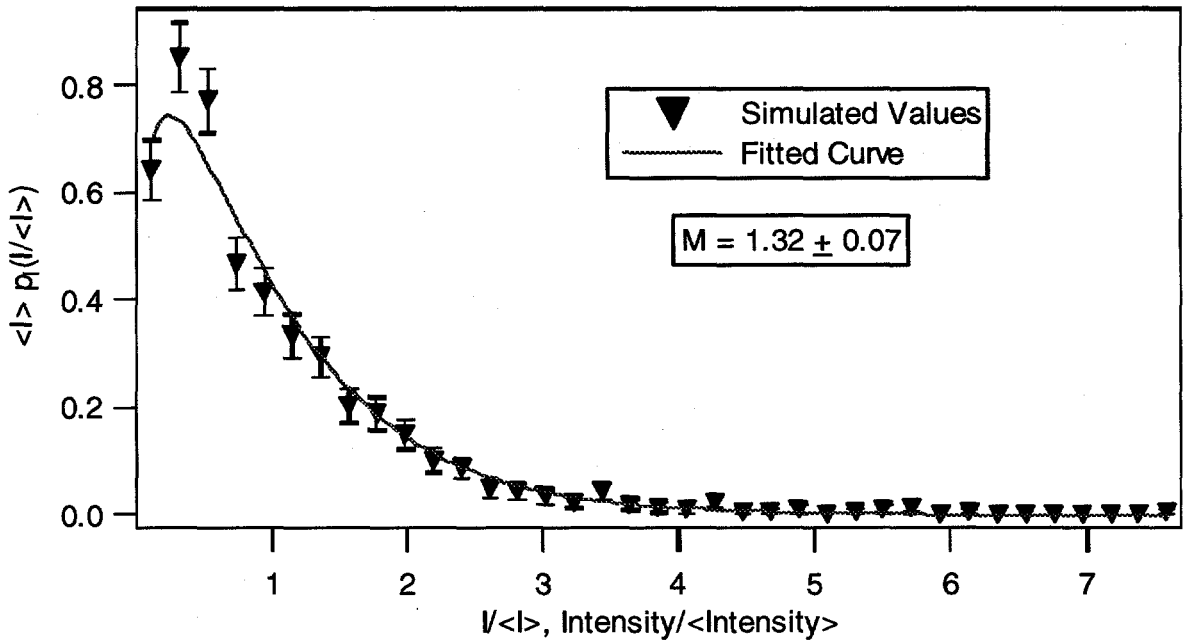

Figure 12. Simulated probability density function for a receiver of radius ~1.7 cm with independent speckle realizations and near zero turbulence ($C_n^2=1\cdot10^{-19}$ $m^{-2/3}$). z = 3300 m. Diffraction limited diameter of beam on target ~0.54 m. The error bars represent the distribution of simulated received intensity for 1000 pulses. The solid curve represents the best fit Gamma distribution. The simulation used five propagation steps on a 512 x 512 array.

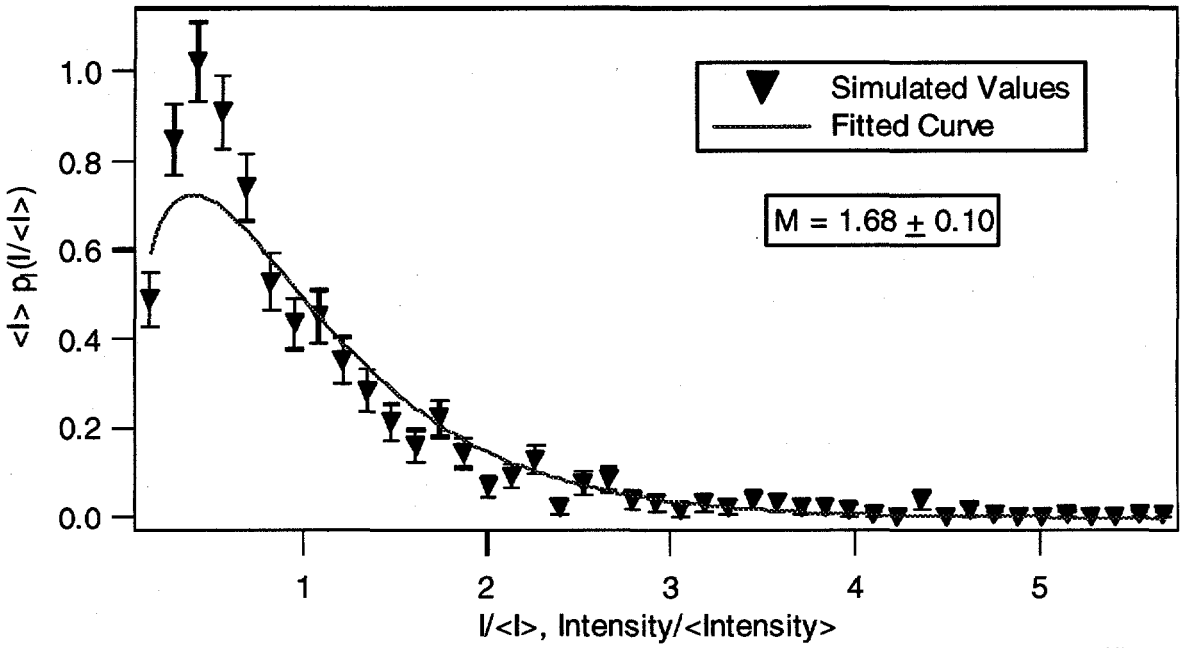

Figure 13. Same simulation parameters as Figure 12 except a higher turbulence level (C_n^2=2·10^{-13} m$^{-2/3}$) Note the transition toward an appearance more like the M=2 case shown in Figure 6.

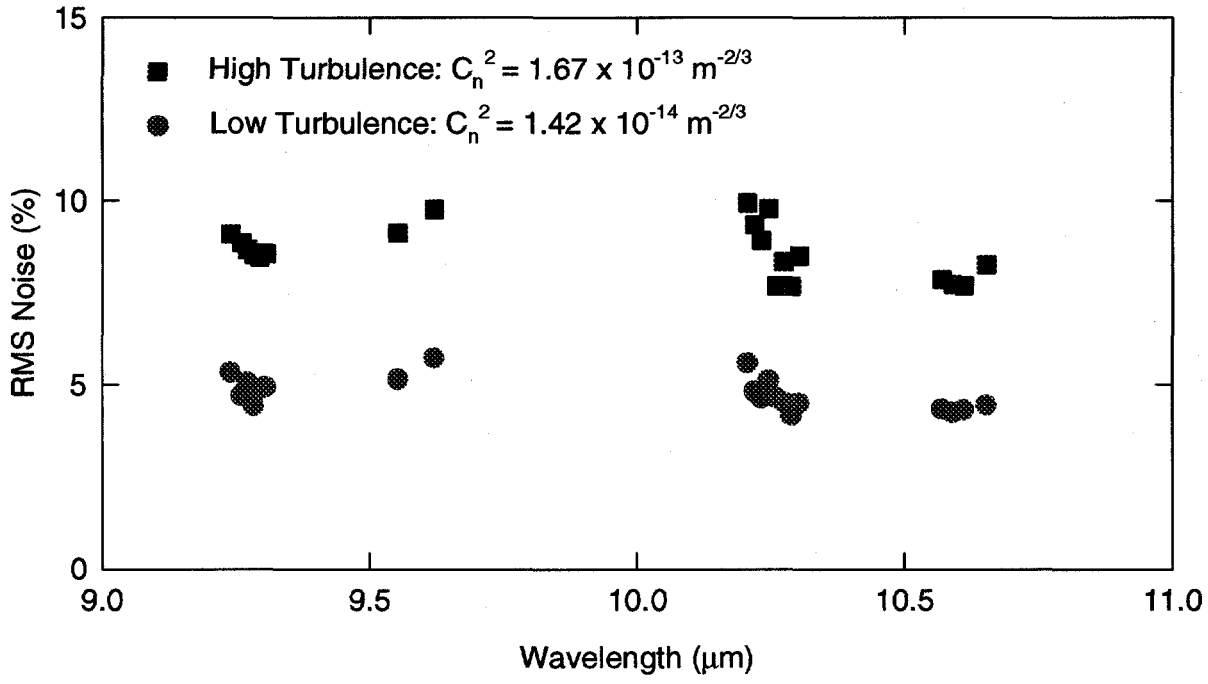

Figure 14. Noise measured for a propagation path of 3390 m, a beam divergence of 1.60 mrad and several CO_2 wavelengths.

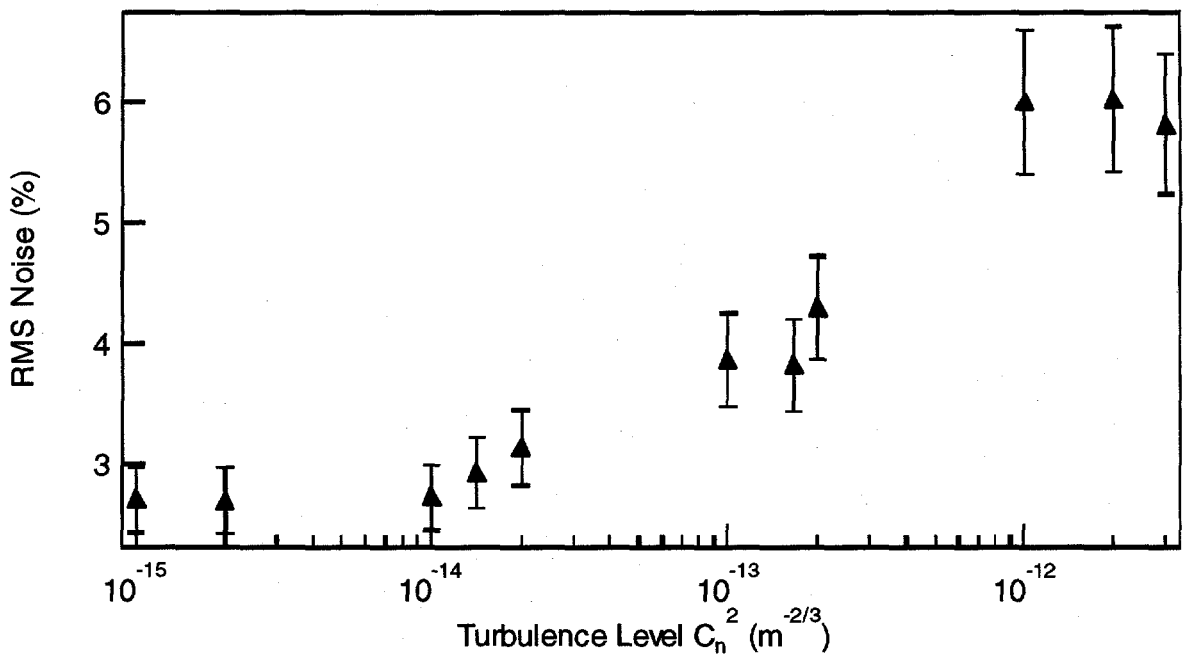

Figure 15. Simulated noise for the LIDAR geometry in Figure 14. The simulation used five propagation steps on a 1024 x 1024 array and averaged over 100 pulses for each turbulence level. The noise level shown here neglects all sources of noise except those due to reflective speckle (independent realizations for each pulse) and atmospheric optical turbulence.

6. REFERENCES

[1] C. Davis, "Computer simulation of wave propagation through turbulent media," Ph.D. Dissertation, Naval Postgraduate School, June 1994.

[2] J. Martin and S. Flatte', "Simulation of point-source scintillation through three-dimensional random media," J. Opt. Soc. Am. A, Vol. 7, No. 5, pp. 838-847, 1990.

[3] R. Petrin, D. Nelson, M. Schmitt, C. Quick, J. Tiee and M. Whitehead, "Atmospheric effects on CO_2 differential absorption lidar sensitivity," *Gas and Chemical Lasers*, R. Sze, Ed., Vol. 2702, pp. 28-39, SPIE, Bellingham, WA, 1996.

[4] IGOR Pro, Version 3.10, WaveMetrics, Inc., Lake Oswego, OR, 1997.

[5] R. Beland, "Propagation through atmospheric turbulence," *The Infrared Electro-optical Systems Handbook*, Vol. 2, SPIE, Bellingham, WA, pp. 157-232, 1993.

[6] R. Fante, "Electromagnetic beam propagation in a turbulent media," Proc. IEEE, Vol. 63, pp. 1669-1692, December 1975.

[7] E. MacKerrow and M. Schmitt, "Measurement of integrated speckle statistics for CO_2 lidar returns from a moving, nonuniform, hard target," Applied Optics, Vol. 36, No. 27, pp. 6921-6937.

[8] J. Russ, *The Image Processing Handbook*, Chapter 4, CRC Press, Boca Raton, FL, 1992.

[9] J. Goodman, "Statistical properties of laser speckle patterns," *Laser Speckle and Related Phenomena*, 2nd ed,. J. Dainty, Ed., Springer-Verlag, New York, 1984.

[10] J. Goodman, *Statistical Optics*, Wiley, New York, 1985.

[11] J. Simonoff, *Smoothing Methods in Statistics*, Chapter 2, Springer-Verlag, New York, 1996.

[12] MATHCAD PLUS 6.0, MathSoft Inc., Cambridge, MA, 1995.

[13] P. Bevington and D. Robinson, *Data Reduction and Error Analysis for the Physical Sciences*, 2nd Ed., pp. 17-95, McGraw-Hill, New York, 1992.

[14] J. Holmes, "Speckle propagation through turbulence: its characteristics and effects," Proc. SPIE, Vol. 410, pp. 89-97, 1983.

[15] MATLAB, Version 5, The MathWorks, Inc., Natick, MA, December 1996.